A Cooperation Control for Multiple Urban Regions Traffic Flow Coupled With an Expressway Network

Yunran Di, Weihua Zhang, Heng Ding, Haotian Shi, Junwei You, Hangyu Li, *Graduate Student Member, IEEE*, and Bin Ran

***Abstract*—As cities expand and long-distance travel demand increases, expressways are usually constructed to enhance regional connectivity. In the mixed road networks of urban roads and expressways, coordinating the distinct traffic dynamics of the two networks is a challenge. To address this challenge, we propose a cooperative flow control method for large-scale mixed networks. First, we develop an integrated traffic model that models urban regions using the macroscopic fundamental diagram (MFD) and expressways using the multi-class cell transmission model (CTM), achieving route tracking of vehicles throughout the entire mixed network. Next, a route choice model is developed to allocate new traffic demands within the mixed network. To coordinate traffic flow, a perimeter control (PC) is conducted to manage transfer flows between region boundaries, ramp metering (RM) to regulate flows entering expressways from urban regions, and variable speed limit (VSL) to control mainline speeds on expressways. We establish this cooperative flow control method within a model predictive control (MPC) framework. Case studies show that, based on the implementation of PC, the combined application of RM and VSL to the expressway system is more effective in reducing congestion and improving traffic efficiency in the mixed network than using RM and VSL independently.**

***Index Terms*—Mixed road networks, macroscopic fundamental diagram, dynamic network models, cooperative flow control.**

I. Introduction

A. Background

URBANIZATION and economic growth have driven the rapid expansion of modern metropolises, resulting in dispersed urban structures, longer travel distances, increased car usage, and worsening congestion [1]. To accommodate the growing travel demand, many cities have constructed large-scale expressway systems [2]. For example, metropolises such as Beijing, Tokyo, and Moscow have developed ring-radial expressway networks to enhance connectivity between urban cores and surrounding areas [3], [4], [5]. The expansion of these infrastructures has transformed urban transportation into a mixed network comprising urban roads and expressways, resulting in complex traffic flow interactions.

In a mixed network, traffic network complexity increases significantly. Compared to traditional urban road networks, mixed networks offer more travel options, allowing vehicles to navigate within urban areas or utilize expressways to traverse multiple regions. This results in more complex route choices, requiring travelers to weigh the trade-offs between urban roads and expressway corridors. Meanwhile, traffic flow exchanges become more intricate, involving multi-level interactions between regions, between regions and expressways, and between expressways themselves. Such interactions intensify network coupling, where congestion in one subsystem can propagate through ramps to another, exacerbating overall traffic pressure. Therefore, to address these complex traffic flow interactions, optimizing and controlling traffic flow is crucial for alleviating network congestion.

Current traffic control strategies primarily focus on optimizing either urban roads or expressways independently. For expressways, common approaches include variable speed limits (VSL) and ramp metering (RM). VSL adjusts mainline speeds via variable message signs to mitigate congestion at bottlenecks [6], [7], [8], while RM regulates on-ramp inflows to reduce merging conflicts [9], [10]. For urban regions, many control strategies are proposed based on the macroscopic fundamental diagram (MFD). MFD is a tool for characterizing large-scale urban networks by describing network-wide traffic behavior under varying density and flow conditions. The theoretical concept of MFD was introduced by Daganzo [11] and empirically validated by Geroliminis and Daganzo [12]. It provides a simplified representation of network-wide traffic characteristics, supporting various modeling approaches based on accumulation, trips, or delays [11], [13], [14], [15], thereby offering a theoretical foundation for traffic control optimization. The main MFD-based control strategies that have been proposed include route guidance [16], [17], [18], [19], congestion pricing [20], [21], [22] and perimeter control (PC) [23], [24], [25]. Route guidance improves network efficiency by providing optimized

Received 10 October 2024; revised 9 May 2025; accepted 15 June 2025. Date of publication 20 June 2025; date of current version 27 October 2025. This work was supported in part by the National Natural Science Foundation of China under Grant 52072108 and Grant 52372326, in part by the Municipal Natural Science Foundation of Hefei under Grant 2022020, and in part by the China Scholarship Council Awards. Recommended for acceptance by Prof. Eirini Eleni Tsiropoulou. *(Corresponding authors: Heng Ding; Haotian Shi.)*

Yunran Di is with the College of Civil Engineering, Hefei University of Technology, Hefei 230009, China (e-mail: diyunran@mail.hfut.edu.cn).

Weihua Zhang and Heng Ding are with the School of Automotive and Traffic Engineering, Hefei University of Technology, Hefei 230009, China (e-mail: weihuazhang@hfut.edu.cn; dingheng@hfut.edu.cn).

Haotian Shi is with the College of Transportation, Tongji University, Shanghai 201804, China (e-mail: shihaotian95@tongji.edu.cn).

Junwei You, Hangyu Li, and Bin Ran are with the Department Civil and Environmental Engineering, University of Wisconsin-Madison, Madison, WI 53706 USA (e-mail: jyou38@wisc.edu; hli939@wisc.edu; bran@wisc.edu).

Digital Object Identifier 10.1109/TNSE.2025.3580759

travel recommendations, congestion pricing dynamically adjusts tolls to reduce peak-hour demand, and PC regulates interregional traffic exchange to alleviate congestion in urban core areas.

However, these methods primarily optimize individual subsystems without fully accounting for the interactions between expressways and urban roads in mixed networks. Since urban roads and expressways are interdependent yet distinct subsystems, independent control strategies may lead to unbalanced traffic distribution, exacerbating congestion in certain areas. Such fragmented control approaches can reduce overall traffic efficiency. For instance, while ramp metering can prevent excessive congestion on expressways, it may result in long queues at on-ramps, disrupting the stability of urban road operations. Therefore, mixed networks require coordinated control strategies to harmonize traffic flow between subsystems and improve overall traffic performance.

Despite the potential benefits of coordinated control, its implementation in large-scale mixed networks poses significant challenges. As network size expands, traffic flow interactions, route choice complexity, and the number of control nodes increase, making global optimization more difficult. Therefore, developing an effective modeling approach and implementing coordinated control for large-scale mixed networks is a critical issue. To address this challenge, this study proposes a modeling and coordinated control framework for multi-region coupled expressway networks, overcoming the limitations of existing methods in large-scale traffic systems. After reviewing related studies, the paper will present the main works and contributions.

TABLE I
COMPARISON OF RELATED STUDIES

Authors	Control Scope	Expressway Modeling	Urban road Modeling	Control Strategy
Ma et al. (2025)	Local control	Microscopic model	Microscopic model	Trajectory control
Deng et al. (2023)	Local control	Microscopic model	Microscopic model	Signal control
Su et. al (2014)	Local control	Microscopic model	Microscopic model	Signal control and RM
Xu et al. (2024)	Local control	Microscopic model	Microscopic model	Signal control and RM
Farabi et al. (2024)	Local control	CTM	CTM	Signal control and RM
Han et al. (2024)	Local control	Microscopic model	Microscopic model	Signal control and RM
Haddad et al. (2013)	Macro control	CTM	MFD	PC and RM
Ding et al. (2020)	Macro control	CTM	MFD	PC, RM and route guidance
Hu and Ma (2024)	Macro control	CTM	MFD	PC and RM
Wang and Gayah (2021)	Macro control	Point queue model	MFD	Pricing

B. Related Studies

Some most relevant studies on mixed networks traffic control are summarized in Table I, categorized by control scope into local control and macro control. Existing researches on coordinated urban networks and expressways mostly focuses on local control of on/off ramps and adjacent intersections. For example, Ma et al. [26] optimized the merging of vehicles at off-ramps and urban roads, addressing weaving conflicts. Deng et al. [27] focused on optimizing signal timing at the intersections of off-ramps, improving traffic flow. Meanwhile, Su et al. [28] and Xu et al. [29] both proposed coordinated control strategies combining signal optimization and ramp metering to enhance the flow between urban expressways and adjacent intersections. These methods employ microscopic modeling approaches to represent traffic scenarios. In contrast, Farabi et al. [30] utilized the cell transmission model (CTM) [31] for traffic modeling at intersections and on-ramps, conducting local coordinated control studies. However, local control may not effectively alleviate congestion in large-scale mixed networks, as the modeling methods and control strategies used often face scalability issues when applied to networks with thousands of roads.

Compared to local control, macro coordination control methods are better suited for alleviating congestion in large-scale networks. However, despite their advantages, research in macro coordination control remains limited. For instance, Haddad et al. [32] used an asymmetric CTM model to study a mixed network comprising two adjacent urban regions and one expressway, implementing coordinated control through PC at the urban region boundaries and RM at on-ramps to optimize traffic flow distribution. Later, Ding et al. [33] combined CTM and MFD models, proposing a control method based on route guidance, PC, and RM to improve traffic coordination. In addition, Wang et al. [34] proposed an optimal control method for congestion pricing for a scenario with two regions and an expressway to improve traffic performance while maximizing revenue.

With rapid advancements in artificial intelligence and machine learning, these techniques have been widely adopted in traffic flow estimation and control, particularly for expressways and urban networks. For traffic prediction, convolutional neural networks have been employed to estimate real-time traffic density from video feeds, dynamically guiding intersection signal strategies [35]. Azimjonov et al. used Yolov5 for accurate nighttime highway traffic estimation [36], while Fernández-Sanjurjo et al. developed a deep learning-based vision system applicable to urban roundabouts and expressways [37]. Khan et al. also proposed an image-based machine learning method to enhance expressway traffic prediction [38]. In terms of traffic control, reinforcement learning (RL) is increasingly utilized for intelligent signal optimization. Han et al. proposed an adaptive RL method using a parameterized deep Q-network for cooperative intersection control [39]. Choe et al. introduced a multi-agent RL framework for city-level coordinated traffic signals [40]. Han et al. [41] proposed a RL-based approach to simultaneously optimize signal control and ramp metering, enabling more intelligent

traffic management. In addition, Genders et al. applied RL with linear function approximation for real-time signal optimization [42], and Hu and Ma developed a demonstration-guided deep RL method integrating PC and RM for large-scale network coordination [43]. Despite their advantages in responsiveness and adaptability, purely data-driven methods face significant difficulties in mixed road networks. These networks consist of different subsystems—urban regions and expressways—that have distinct traffic patterns and structural features. Moreover, the connection between them often occurs through ramps, where congestion and queuing can easily spread from one part of the network to another. This kind of complex interaction is difficult for data-driven models to capture accurately, especially when the training data is limited or lacks diversity. In response to these challenges, recent studies have consistently demonstrated the effectiveness of combining the CTM and MFD in modeling and controlling mixed networks [32], [33], [34], [44]. Motivated by these findings, this study extends the CTM–MFD hybrid framework to model traffic dynamics in large-scale networks comprising multiple urban regions and expressways.

Although recent studies have made notable progress in applying CTM–MFD hybrid frameworks to mixed network modeling and control, their application to large and complex networks remains limited. In particular, existing methods do not fully capture critical traffic interactions at the network level. (1) Current traffic models for mixed networks often ignore the flow transfer between interconnected expressways, focusing only on the flow between urban regions and expressways. In many cities, expressways have already formed circular-radial network structures, and traffic flow between expressways via interchanges constitutes a significant part of overall dynamics. However, this process is normally neglected due to the complexity of constructing models for expressway networks. (2) Although the cooperative strategy combining PC and RM mentioned previously has the potential to reduce traffic congestion on mixed networks, it still has limitations. Both PC and RM focus on restricting flows at the boundary between two control objects—PC at regional boundaries and RM at on-ramps—but such boundary flow control inevitably leads to vehicle queues. Especially for RM, the limited length of on-ramps can cause queue spillback and raise safety concerns [45]. (3) Current research has not fully considered the impact of ramp metering queues on urban network traffic states. In practice, when on-ramp queues are too long, they may extend into urban regions, but this interaction is rarely captured in existing traffic state prediction models.

In light of these limitations, developing a comprehensive traffic model for mixed networks and designing effective coordinated control methods face several key challenges. (1) Complex flow transfer processes: Mixed networks involve complicated traffic dynamics, including not only flows between urban regions and expressways but also frequent exchanges between expressways themselves. Accurately modeling these multi-directional flow transfers is a major challenge. (2) Route choice in large-scale networks: Large-scale mixed networks involve numerous traffic entities, including multiple urban regions and expressways. Each vehicle's route selection may involve multiple regions and expressways simultaneously, making it difficult to predict travel times and make route choices. (3) Coordinated control across multiple entities: With multiple urban regions and expressways intersecting, existing control methods may not fully address the global regulation requirements. Given the complexity of mixed networks, control strategies may need to be expanded to enable more coordinated traffic management across the entire network.

C. Main Works and Contributions

Based on the above-identified research gaps and challenges, we propose a cooperative control approach for a network combining multiple urban regions and expressways to address gaps in mixed network studies. The control method consists of two main components: 1) developing a traffic model for mixed networks and 2) establishing a cooperative control model.

Regarding traffic modeling, we use a combination of CTM and MFD methods to enhance the mixed network traffic model in the following ways. First, we design a method for dividing expressway networks in a mixed network. This method includes configuring on-ramps and off-ramps to connect the expressways with connected regions, as well as implementing connecting ramps to establish direct links between connected expressways, ensuring smooth transitions for vehicles across all interconnected traffic entities. Next, while using the MFD to describe regional dynamics, we utilize multi-class CTM to track vehicle routes within the expressway network, achieving more accurate flow predictions. Additionally, we model the queueing at the boundaries of the mixed network, providing a more realistic depiction of how expressway flow control affects the states of interconnected regions.

Regarding traffic control, considering the relatively long mainline segments of expressways, VSL can adjust vehicle speeds to regulate flow and provide greater storage capacity for vehicles during congestion. However, VSL alone may be insufficient to manage sudden surges of traffic demand. In contrast, RM effectively limits the inflow of vehicles from on-ramps but may cause excessive queueing when used alone. To leverage the advantages of both methods, this study proposes a cooperative control model that integrates PC, RM, and VSL. This model is developed within a model predictive control (MPC) framework to alleviate congestion in the mixed network.

The contributions of this paper are as follows:

1) A macro traffic model for mixed networks is developed, enabling vehicle transfers among all interconnected traffic entities and introducing a queueing mechanism at boundaries. This approach fully considers congestion spillback effects at ramps and regional boundaries, allowing for a more accurate description of the impact of flow control on the overall network. It provides a reliable foundation for assessing traffic states for coordinated control.
2) To address the complex traffic interactions between expressway networks and urban regions, a cooperative control strategy is proposed, combining PC, RM, and VSL. This strategy facilitates dynamic optimization across the entire network, enhancing the coordination of traffic flow among all interconnected traffic entities.

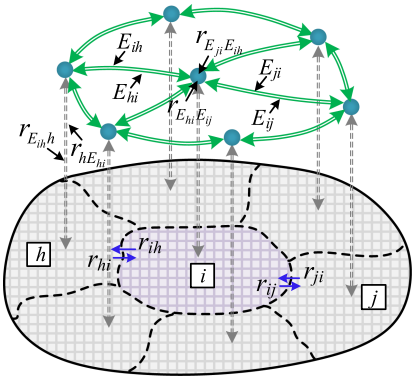

Fig. 1. Layout pattern of mixed network.

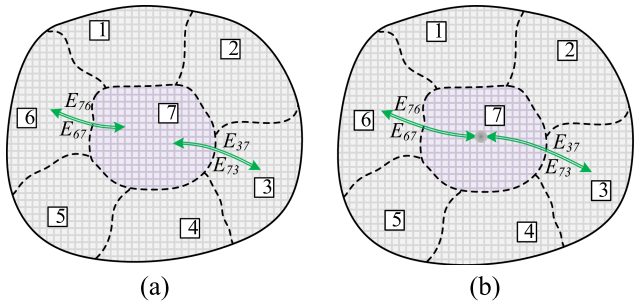

Fig. 2. (a) No direct connections between different expressways; (b) Direct connections between expressways passing through the same region.

D. Organization

The remaining sections are summarized below. Section II describes the research problem. Section III develops the traffic model for the mixed network. Section IV proposes the cooperative control method, and Section V presents the results of the case study. In the last section, conclusions are drawn, and future work is summarized.

II. Problem Description

A. Scenario Description of Mixed Road Network

Consider a large-scale mixed network consisting of an urban network and an expressway network, where the urban network has been divided into several regions, as shown in Fig. 1. Therefore, there may be an expressway as an alternative route between adjacent regions. Due to the long span of expressways, one may run through several regions. For modeling purposes, we treat expressways connecting any adjacent region separately so that the expressway network is divided into sections. Since the expressway has two opposite travel directions, the expressway from region i to the adjacent region j is defined as E_{ij}, $i \neq j$.

In a mixed network, traffic can be transferred between neighboring regions through boundaries. Let r_{ij} denote the boundary from region i to adjacent region j. Whereas traffic flows are transferred between expressways and urban regions through on-ramps and off-ramps. Since expressway networks involve numerous parameters, including the number and location distribution of ramps, the following assumptions are given to simplify the road network structure and route choice:

i) Each expressway has only one on-ramp and one off-ramp connected to the urban network. That is, if there exists an expresswayE_{ij}, then E_{ij} has only one on-ramp in the origin region i and only one off-ramp in the termination region j. Denote $r_{iE_{ij}}$ as the on-ramp between expressway E_{ij} and region i, and $r_{E_{ij}j}$ as the off-ramp between expressway E_{ij} and region j;

ii) When there are multiple expressways connecting the same region, these expressways will intersect with each other. As shown in Fig. 1, given a region i, if both expressway E_{hi} and expressway E_{ij} exist, a connecting ramp $r_{E_{hi}E_{ij}}$ will be provided to facilitate traffic directly transitioning from expressway E_{hi} to expressway E_{ij} without passing through region i.

iii) Vehicles are allowed to make a maximum of one transfer within the same region (expressway) during each trip; they are not allowed to leave a region (an expressway) and then return to it.

Regarding (i), although the case of a single expressway with multiple ramps is not considered, this assumption reflects the structural characteristics of a mixed network and simplifies route selection. Assumption (ii) is based on practical considerations. Vehicle travel within the expressway system requires interchanges between different expressways to enhance connectivity and accessibility of the expressway network. An example is used for comparison. In the scenario shown in Fig. 2(a), there is no connection established between different expressways. Therefore, the route from region 6 to region 3 via the expressways is 6→E_{67}→7→E_{73}→3. Here, the transfer from expressway E_{67} to E_{73} must pass through region 7. However, in Fig. 2(b), the connecting ramp directly links E_{67} and E_{73}, enabling a shorter route 6→E_{67}→E_{73}→3, thus avoiding unnecessary traversal of region 7. The scenario in Fig. 2(b) enriches the travel options and better reflects actual travel patterns and infrastructure design. Finally, assumption (iii) is made to reduce invalid routes and align with real-world travel habits.

B. Research Framework

Based on the scenario description, a mixed network can be viewed as coupling multiple urban regions and an expressway network. In a mixed network, each region and expressway can be regarded as a macro node along the route. The structure of the mixed network is represented as $G = (R, N, C)$, where R denotes the set of regions, $R = \{1, \ldots, i_m\}$, and i_m is the total number of regions; N denotes the set of expressways, $N = \{E_{ij}\}$, $i \neq j$; and C represents the set of links connecting any two adjacent nodes in the route with $C = \{r_{ij}, r_{iE_{ij}}, r_{E_{hi}i}, r_{E_{hi}E_{ij}}\}$.

The issue addressed in this paper is to propose a control method for large-scale mixed networks. PC, RM, and VSL can be employed to regulate traffic flow cooperatively. Fig. 3 illustrates the research framework, which mainly includes two parts: 1) constructing a mixed network traffic model and 2) proposing a cooperative control scheme. First, we use the MFD

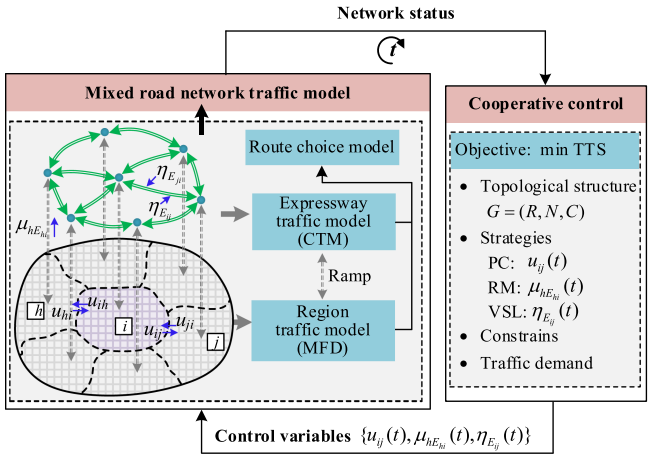

Fig. 3. Research framework.

to describe the dynamics of traveling accumulation $n^{\rho}_{i,T}(t)$ and queueing accumulation $n^{\rho}_{i,Q}(t)$ for multi-region urban networks, while using the CTM to model traffic density on expressways, including mainline density $K_{E_{ij},l_{ij}}(t)$, and ramp density $K_{iE_{ij}}(t)$, $K_{E_{ij}j}(t)$ and $K_{E_{hi}E_{ij}}(t)$. Then, a route choice model is established by predicting the travel time on the routes. Finally, using the mixed network traffic model as a forecasting tool, we propose an MPC-based cooperative control to minimize the total time spent (TTS) of vehicles in the road network. This strategy optimizes and generates the optimal perimeter control rate $u_{ij}(t)$, ramp metering rate $\mu_{iE_{ij}}(t)$, and variable speed limit $\eta_{E_{ij}}(t)$ to be applied to the mixed network, aiming to minimize overall network congestion. The following sections will detail this methodology with explanations.

III. Traffic Flow Model of Mixed Network

This section introduces the mixed network traffic model. We conduct traffic modeling separately for both regions (using MFD) and expressway networks (using CTM), and based on this, we develop a route choice model. For ease of distinction, define α_i as the set of immediately neighboring regions of region i, and β_i as the set of regions that can be connected to region i through an expressway.

A. MFD-Based Traffic Model for Urban Regions

First, we introduce the MFD-based region traffic model. Daganzo [11] and Geroliminis and Daganzo [12] developed the accumulation-based MFD, which provides the relationship between production and the accumulation of vehicles for a homogeneously congested urban network. Consider a homogeneous region $i \in R$ with travel production MFD $P_i(n_i(t)) = n_i(t) \cdot v(n_i(t))$, where $n_i(t)$ and $v_i(t)$ are the accumulation of vehicles and the average travel speed in region i at time t, respectively. We treat each region and expressway in the mixed network as a macro node; therefore, each route can be viewed as a sequence of nodes arranged in the order of travel from the origin to the destination. Since vehicles generate and exit within the urban network, the origin and destination nodes must be regions, while the other nodes can be either regions or expressways. Let $n^{\rho}_i(t)$ denote the accumulation of vehicles in region i at time t with routeρ, thus $n_i(t) = \sum_{\rho} n^{\rho}_i(t)$.

In the mixed network, not all vehicles completing their trips within a region can immediately transfer to an adjacent region or connecting expressway because of flow restrictions and capacity limitations. Vehicles that cannot transfer immediately will have to wait at the boundary or before the on-ramp, resulting in a queue. Therefore, the accumulation $n^{\rho}_i(t)$ within any region i can be divided into (i) traveling accumulation $n^{\rho}_{i,T}(t)$ and (ii) queueing accumulation $n^{\rho}_{i,Q}(t)$. Let $n_{i,T}(t)$ and $n_{i,Q}(t)$ denote the total traveling accumulation and queueing accumulation in region i, the total accumulation $n_i(t)$ in region i at time t can be estimated as:

$$n_i(t) = n_{i,T}(t) + n_{i,Q}(t) = \sum_{\rho} n^{\rho}_{i,T}(t) + \sum_{\rho} n^{\rho}_{i,Q}(t) \quad (1)$$

Supposing a constant trip length in urban region i, the trip completion rate for traveling accumulation $n^{\rho}_{i,T}(t)$ at time t is:

$$m^{\rho}_i(t) \approx \frac{n^{\rho}_{i,T}(t)}{n_i(t)} \cdot \frac{P_i(n_i(t))}{\bar{L}_i} \quad (2)$$

where $\bar{L}_i$ is the average trip length for vehicles in region i.

Vehicles that have completed their trips in the region will be excluded from the MFD dynamics and wait to transfer to the next node. Note that there is no queuing for exit flow within the region, as no limitations are imposed. Let $\rho(-i)$ and $\rho(+i)$ denote the previous and the next node of the region i in the route ρ, respectively. Donate $f^{\rho}_{i\to\rho(+i)}(t)$ as the transferring demand from region i to node $\rho(+i)$ at the boundary or before the on-ramp. If $\rho(+i)$ is a region j, during the simulation time interval T_s, the transferring demand from region i to region j with route ρ is $f^{\rho}_{i\to j}(t) = n^{\rho}_{i,Q}(t)/T_s$. The transferring demand $f^{\rho}_{i\to j}(t)$ is restricted by the boundary capacity and receiving capacity of region j [38]. Therefore, the restricted transferring flow from region i to region j is the minimum of (i) the transferring demand $f^{\rho}_{i\to j}(t)$, (ii) the fraction of the boundary capacity from region i to region j that is assigned to $f^{\rho}_{i\to j}(t)$, and (iii) the fraction of the receiving capacity of region j that is assigned to $n^{od,p}_{i\to j}(t)$, as shown in the following:

$$\hat{f}^{\rho}_{i\to j}(t) = \min\left\{ f^{\rho}_{i\to j}(t), \frac{f^{\rho}_{i\to j}(t)}{\sum_x f^{x}_{i\to j}(t)} \cdot b_{ij}, \frac{f^{\rho}_{i\to j}(t)}{\sum_{s\in\alpha_j}\sum_x f^{x}_{s\to j}(t) + \sum_{h\in\beta_j}\sum_x \delta^{x}_{E_{hj}j}(t)} \cdot c_i(n_{j,T}(t)) \right\} \quad (3)$$

where $f^{x}_{i\to j}(t)$ is the transferring demand from region i to region j with route x; b_{ij} is the boundary capacity from region i to region j; $f^{x}_{s\to j}(t)$ is the transferring demand from region s to region j with route x; $\delta^{x}_{E_{hj}j}(t)$ is the sending flow of off-ramp $r_{E_{hj}j}$ with route x, which will be estimated via CTM theory;

$c_j(n_{j,T}(t))$is the receiving capacity of region j defined as [46]:

$$c_i(n_{j,T}(t)) = c_{j,\max} \cdot \left(1 - \frac{n_{j,T}(t)}{n_{j,\text{jam}}}\right) \tag{4}$$

where $c_{j,\max}$ and $n_{j,\text{jam}}$ are the maximum receiving capacity and jam accumulation of region j, respectively. As the type of queue in this paper is described using a point queue model that does not occupy any physical space [47], queuing accumulation does not influence the region's receiving capacity.

If the next node$\rho(+i)$ is an expresswayE_{ij}, the transferring demand from region i to expressway E_{ij} with route ρ is $f^{\rho}_{i\to E_{ij}}(t) = n^{\rho}_{i,Q}(t)/T_s$. The transferring demand $f^{\rho}_{i\to E_{ij}}(t)$ will be restricted by the receiving capacity of on-ramp$r_{iE_{ij}}$, and the restricted transferring flow is estimated as:

$$\hat{f}^{\rho}_{i\to E_{ij}}(t) = \min\left\{ f^{\rho}_{i\to E_{ij}}(t), \frac{f^{\rho}_{i\to E_{ij}}(t)}{\sum_x f^{x}_{i\to E_{ij}}(t)} \cdot \zeta_{iE_{ij}}(t) \right\} \tag{5}$$

where $f^{x}_{i\to E_{ij}}(t)$ is the transferring demand from region i to expressway E_{ij} with route x; $\zeta_{iE_{ij}}(t)$ is the receiving flow of on-ramp $r_{iE_{ij}}$.

Depending on the route and node where the vehicle is located, the dynamic state equations for $n^{\rho}_{i,T}(t)$ and $n^{\rho}_{i,Q}(t)$ are:

$$\frac{dn^{\rho}_{i,T}(t)}{d(t)} = \begin{cases} q^{\rho}_{od}(t) - m^{\rho}_{i}(t) & \text{(i) } i = o \\ u_{hi}(t)\cdot \hat{f}^{\rho}_{h\to i}(t) - m^{\rho}_{i}(t) & \text{(ii) } i \neq o \ \&\ \rho(-i) = h \\ Q^{\rho}_{E_{hi}i}(t) - m^{\rho}_{i}(t) & \text{(iii) } i \neq o \ \&\ \rho(-i) = E_{hi} \end{cases} \tag{6}$$

$$\frac{dn^{\rho}_{i,Q}(t)}{d(t)} = \begin{cases} m^{\rho}_{i}(t) - u_{ij}(t)\cdot \hat{f}^{\rho}_{i\to j}(t) & \text{(i) } \rho(+i) = j \\ m^{\rho}_{i}(t) - \hat{f}^{\rho}_{i\to E_{ij}}(t) & \text{(ii) } \rho(+i) = E_{ij} \end{cases} \tag{7}$$

where $u_{hi}(t)$ and $u_{ij}(t)$ are the PC rates at boundaries r_{hi} and r_{ij}, respectively; $Q^{\rho}_{E_{hi}i}(t)$ is the traffic flow in off-ramp $r_{E_{hi}i}$ with route ρ; $q^{\rho}_{od}(t)$ is the part of the newly generated traffic demand $q_{od}(t)$ from region o to region d that is assigned to route ρ.

B. CTM-Based Traffic Model for Expressway Network

For the expressway network, we propose a CTM-based traffic model. The expressway division in the mixed network is shown in Fig. 4. Based on the CTM theory, every expressway is divided into cells according to the traveling direction and the length of each cell is L_s. Denote $s_{E_{ij},l_{ij}}$ as a mainline cell on the expressways E_{ij},$l_{ij} \in [1, L_{ij}]$. When there are expressways E_{hi} and E_{ij} intersecting in region$i$, connecting ramp $r_{E_{hi}E_{ij}}$ will be provided to realize interchange between expressways. For simplicity, the ramps are all a cell of length L_s. Donate the traffic densities of mainline cell $s_{E_{ij},l_{ij}}$, on-ramp cell $r_{iE_{ij}}$, off-ramp $r_{E_{ij}j}$ and connecting ramp $r_{E_{hi}E_{ij}}$ are $K_{E_{ij},l_{ij}}(t)$, $K_{iE_{ij}}(t)$, $K_{E_{ij}j}(t)$ and $K_{E_{hi}E_{ij}}(t)$, respectively. For a more accurate traffic flow prediction, multi-class CTM is used to distinguish and track traffic flows with different routes within the expressway networks [48]. Let $K^{\rho}_{E_{ij},l_{ij}}(t)$ be the traffic density in cell $s_{E_{ij},l_{ij}}$ with route ρ, thus$K_{E_{ij},l_{ij}}(t) = \sum_\rho K^{\rho}_{E_{ij},l_{ij}}(t)$. Similarly, $K^{\rho}_{iE_{ij}}(t)$, $K^{\rho}_{E_{ij}j}(t)$ and $K^{\rho}_{E_{hi}E_{ij}}(t)$ are donated as the traffic densities in cell $r_{iE_{ij}}$, $r_{E_{ij}j}$ and $r_{E_{hi}E_{ij}}$ with route ρ.

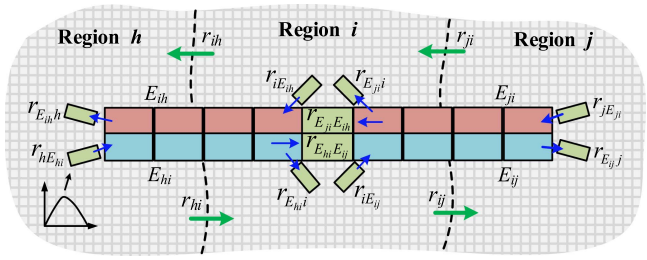

Fig. 4. Diagram of expressway division in the mixed network.

The CTM usually defines the sending and receiving flows of a cell by using a triangular fundamental diagram (FD) [49]. For the mainline cells, the FD parameters are free-flow speed V_{fm}, the capacity C_m, the congestion wave speed ω_m, and the jam density K_{jm}. For the ramp cells, the FD parameters are free flow speed V_{fr}, the capacity C_r, the congestion wave speed ω_r, and the jam density K_{jr}. The density dynamics for each type of cell, from vehicles entering to exiting the expressway, are established and introduced as follows.

1) On-Ramps: Vehicles leaving the region for the expressway are the first to enter the on-ramps. The sending flow for traffic density $K^{\rho}_{iE_{ij}}(t)$ within the on-ramp $r_{iE_{ij}}$ is:

$$\delta^{\rho}_{iE_{ij}}(t) = \min\{V_{fr}\cdot K^{\rho}_{iE_{ij}}(t), C_r\} \tag{8}$$

The receiving flow of the on-ramp $r_{iE_{ij}}$ is:

$$\zeta_{iE_{ij}}(t) = \min\{\omega_r \cdot (K_{jr} - K_{iE_{ij}}(t)), C_r\} \tag{9}$$

The vehicles that have just left the on-ramp will enter the first mainline cell. If there exists a connected expressway E_{hi}, the traffic demand for E_{ij} comes from both the on-ramp $r_{iE_{ij}}$ and the expressways E_{hi}. Therefore, the traffic flow merging from the on-ramp $r_{iE_{ij}}$ into the mainline is:

$$Q^{\rho}_{iE_{ij}}(t) = \min \left\{ \delta^{\rho}_{iE_{ij}}(k), \frac{\delta^{\rho}_{iE_{ij}}(t)}{\sum_x \delta^{x}_{iE_{ij}}(t) + \sum_{h\in\beta_i}\sum_x \delta^{x}_{E_{hi}E_{ij}}(t)} \cdot \zeta_{E_{ij},1}(t) \right\} \tag{10}$$

where $\zeta_{E_{ij},1}(t)$ is the receiving flow of the first mainline cell of expressway E_{ij}; $\delta^{x}_{iE_{ij}}(t)$ is the sending flow with route x in the on-ramp $r_{iE_{ij}}$; $\delta^{x}_{E_{hi}E_{ij}}(t)$ is the sending flow with route x in the connecting ramp $r_{E_{hi}E_{ij}}$. Additionally, the actual transfer flow of traffic demand $\delta^{x}_{E_{hi}E_{ij}}(t)$ subject to constraints is donated as $Q^{x}_{E_{hi}E_{ij}}(t)$.

The dynamics of a cell are due to the difference between its inflow and outflow. The traffic dynamic of on-ramp $r_{iE_{ij}}$

considering RM constraints is:

$$\frac{dK^{\rho}_{iE_{ij}}(t)}{d(t)} = f^{\rho}_{i\to E_{ij}}(t) - \mu_{iE_{ij}}(t)\cdot Q^{\rho}_{iE_{ij}}(t) \tag{11}$$

where $\mu_{iE_{ij}}(t)$ is the RM rate for on-ramp $r_{iE_{ij}}$ at time t.

2) Mainline: Vehicles in the mainline transfer in the travel direction to the downstream cells. When the VSL controls the mainline cell, the vehicle will be traveling at a limited speed. The sending flow of vehicles with density $K^{\rho}_{E_{ij},l_{ij}}(t)$ and the receiving flow of cell $r_{E_{ij},l_{ij}}$ affected by the VSL control can then be determined as [50]:

$$\delta^{\rho}_{E_{ij},l_{ij}}(t) = \min\{\eta_{E_{ij}}(t)\cdot K^{\rho}_{E_{ij},l_{ij}}(t), C_{vsl}\} \tag{12}$$

$$\zeta_{E_{ij},l_{ij}}(t) = \min\{\omega_m\cdot(K_{jm} - K_{E_{ij},l_{ij}}(t)), C_{vsl}\} \tag{13}$$

where $\eta_{E_{ij}}(t)$ is the speed limit for expressway E_{ij}; C_{vsl} is the maximum flow under the current speed limit.

Expressway merging zones often experience capacity degradation. This paper simulates this phenomenon using the method proposed by Han et al. [49]. If cell $r_{E_{ij},l_{ij}}$ is merging bottleneck, the maximum outflow of cell $r_{E_{ij},l_{ij}}$ is:

$$C^{\max}_{E_{ij},l_{ij}}(t) = min\left\{C_m, C_m\cdot\left(1-\xi\cdot\frac{K_{E_{ij},l_{ij}}(t)-K_{cm}}{K_{jm}-K_{cm}}\right)\right\} \tag{14}$$

where K_{cm} is the critical density, and ξ denotes the maximum extent of the capacity drop.

Let $\rho(-E_{ij})$ and $\rho(+E_{ij})$ denote the previous and next nodes of E_{ij} in the route ρ, respectively. Thus, the traffic flow of the mainline cell $r_{E_{ij},l_{ij}}$ can estimated based on its location and the type of the next node:

$$Q^{od,\rho}_{E_{ij},l_{ij}}(t) = \begin{cases} \min\{\delta^{\rho}_{E_{ij},l_{ij}}(t), \frac{\delta^{\rho}_{E_{ij},l_{ij}}(t)}{\sum_x \delta^{x}_{E_{ij},l_{ij}}(t)}\cdot\zeta_{E_{ij},l_{ij}+1}(t)\} & \text{(i) } l_{ij} < L_{ij} \\ \min\{\delta^{\rho}_{E_{ij},l_{ij}}(t), \frac{\delta^{\rho}_{E_{ij},l_{ij}}(t)}{\sum_x \delta^{x}_{E_{ij},l_{ij}}(t)}\cdot\zeta_{E_{ij}j}(t)\} & \text{(ii) } l_{ij}=L_{ij} \\ & \&\rho(+E_{ij})=j \\ \min\{\delta^{\rho}_{E_{ij},l_{ij}}(t), \frac{\delta^{\rho}_{E_{ij},l_{ij}}(t)}{\sum_x \delta^{x}_{E_{ij},l_{ij}}(t)}\cdot\zeta_{E_{ij}E_{jg}}(t)\} & \text{(ii) } l_{ij}=L_{ij} \\ & \&\rho(+E_{ij})=E_{jg} \end{cases} \tag{15}$$

where $\delta^{x}_{E_{ij},l_{ij}}(t)$ is the sending flow in cell $s_{E_{ij},l_{ij}}$ at time t with route x; $\zeta_{E_{ij}j}(t)$ and $\zeta_{E_{ij}E_{jg}}(t)$ are the receiving flow of the off-ramp $r_{E_{ij}j}$ and the connecting ramp $r_{E_{ij}E_{jg}}$, respectively.

The traffic dynamic of mainline cell $r_{E_{ij},l_{ij}}$ is estimated based on its location and the type of the previous node:

$$\frac{dK^{p}_{E_{ij},l_{ij}}(t)}{d(t)} = \begin{cases} Q^{\rho}_{iE_{ij}}(t) - Q^{\rho}_{E_{ij},l_{ij}}(t) & \text{(i) } l_{ij}=1\,\&\,\rho(-E_{ij})=i \\ Q^{\rho}_{E_{hi}E_{ij}}(t) - Q^{\rho}_{E_{ij},l_{ij}}(t) & \text{(ii) } l_{ij}=1\,\&\,\rho(-E_{ij})=E_{hi} \\ Q^{\rho}_{E_{ij},l_{ij}-1}(t) - Q^{\rho}_{E_{ij},l_{ij}}(t) & \text{(iii) } l_{ij}>1 \end{cases} \tag{16}$$

where $Q^{\rho}_{E_{hi}E_{ij}}(t)$ is traffic flow of the connecting ramp $r_{E_{hi}E_{ij}}$ with route ρ.

3) Off-Ramps: When vehicles travel on the mainline to reach its end, they access the connecting region via the off-ramp. The flow from the off-ramp $r_{E_{ij}j}$ into region j is:

$$Q^{\rho}_{E_{ij}j}(t) = \min\left\{\delta^{\rho}_{E_{ij}j}(t), \frac{\delta^{\rho}_{E_{ij}j}(t)}{\sum_{s\in\alpha_j}\sum_x f^{x}_{s\to j}(t) + \sum_{h\in\beta_j}\sum_x \delta^{x}_{E_{hj}j}(t)}\cdot c_j(n_j(t))\right\} \tag{17}$$

Therefore, the traffic density dynamic of off-ramp $r_{E_{ij}j}$ is:

$$\frac{dK^{\rho}_{E_{ij}j}(t)}{d(t)} = Q^{\rho}_{E_{ij},L_{ij}}(t) - Q^{\rho}_{E_{ij}j}(t), \quad \rho(+E_{ij})=j \tag{18}$$

4) Connecting Ramps: If connecting expressways are available for vehicles on the expressway, they can transfer to the connecting expressways via connecting ramps. The traffic density dynamic of the connecting ramp $r_{E_{hi}E_{ij}}$ is:

$$\frac{dK^{\rho}_{E_{hi}E_{ij}}(t)}{d(t)} = Q^{\rho}_{E_{hi},L_{hi}}(t) - Q^{\rho}_{E_{hi}E_{ij}}(t), \quad \rho(+E_{hi})=E_{ij} \tag{19}$$

C. Route Choice Modeling for Mixed Road Networks

Building on the proposed models for expressways and regions, this section establishes a route choice model for the mixed network. The route choice probability is derived by estimating travel times of all alternative routes between region ODs. Donate Θ_w as the set of all routes between any OD pair w and ρ_w as an alternative route in Θ_w. The total travel time for each route is the sum of travel times at all nodes, so each node's travel time must be evaluated.

For an expressway node, the travel time within the cells can be extrapolated based on the density using CTM. For a region node, the travel time constitutes two terms: (i) inherent regional travel time and (ii) queuing delay at the boundary or on-ramp. The second term is estimated by dividing total queuing accumulation by transferring flow and finding the mean value for any vehicle during any simulation step time interval T_s [51]. Based on this, the travel time of vehicles within region i moving to the next node $\rho(+i)$ via route ρ is:

$$\bar{\tau}^{\rho}_{i\to\rho(+i)}(t) = \frac{\bar{L}_i}{v_i(n_{i,T}(t))} + \frac{1}{2}\frac{\sum_x n^{x}_{i,Q}(t)\cdot\kappa^{x}_{i\rho(+i)}}{T_s\cdot f^{\rho}_{i\to\rho(+i)}(t)} \tag{20}$$

where $\kappa^{x}_{i\rho(+i)}$ is the pre-known parameter: $\kappa^{x}_{i\rho(+i)}=1$ If the next node of region i via route x and ρ are the same (i.e., $x(+i)=\rho(+i)$), and $\kappa^{x}_{i\rho(+i)}=0$, otherwise. Therefore, $\sum_x n^{x}_{i,Q}(t)\cdot\kappa^{x}_{i\rho(+i)}$ is the total queuing accumulation in region i moving to the next node $\rho(+i)$.

Interchanges between nodes in a mixed network may require ramps, and we incorporate the travel time on the ramp passed before entering the node into the total travel time at that node. If a node in the route is region i, considering the types of the previous and next nodes, the total travel time spent for vehicles

passing through region i via route ρ_w is:

$$\tau_i^{\rho_w}(t) = \begin{cases} \bar{\tau}_{i\to j}^{\rho_w}(t) & \text{(i) } \rho_w(-i) \text{ is a region } \& \ \rho_w(+i)=j \\ \bar{\tau}_{i\to E_{ij}}^{\rho_w}(t) & \text{(ii) } \rho_w(-i) \text{ is a region } \& \ \rho_w(+i)=E_{ij} \\ \frac{L_s}{V_{E_{hi}i}(t)}+\bar{\tau}_{i\to j}^{\rho_w}(t) & \text{(iii) } \rho_w(-i)=E_{hi} \,\&\, \rho_w(+i)=j \\ \frac{L_s}{V_{E_{hi}i}(t)}+\bar{\tau}_{i\to E_{ij}}^{\rho_w}(t) & \text{(iv) } \rho_w(-i)=E_{hi} \,\&\, \rho_w(+i)=E_{ij} \end{cases} \tag{21}$$

where $V_{E_{hi}i}(t)$ is the average speed of the off-ramp $r_{E_{hi}i}$. The terms (i) and (ii) in (21) indicate that when the previous node of region i in the route is a region, no ramp travel time should be considered. Whereas the previous node of region i in the terms (iii) and (iv) is an expressway, so the traveling time of the off-ramp should be added.

If the node in the route is an expressway, the total travel time spent for vehicles passing through expressway E_{ij} via route ρ_w is:

$$\tau_{E_{ij}}(t) = \begin{cases} \frac{L_s}{V_{iE_{ij}}(t)} + \sum_{l_{ij}=1}^{L_{ij}} \frac{L_s}{V_{E_{ij},l_{ij}}(t)} & \text{(i) } \rho(-E_{ij})=i \\ \frac{L_s}{V_{E_{hi}E_{ij}}(t)} + \sum_{l_{ij}=1}^{L_{ij}} \frac{L_s}{V_{E_{ij},l_{ij}}(t)} & \text{(ii) } \rho(-E_{ij})=E_{hi} \end{cases} \tag{22}$$

where $V_{iE_{ij}}(t)$ and $V_{E_{hi}E_{ij}}(t)$ are the average speed of on-ramp $r_{iE_{ij}}$ and the connecting ramp $r_{E_{hi}E_{ij}}$, respectively; $V_{E_{ij},l_{ij}}(t)$ is the average speed of the mainline cell $s_{E_{ij},l_{ij}}$.

To relax the assumption that travelers are fully informed about traffic, this paper uses a logit model to simulate the route choice decision based on the more realistic concept of stochastic user equilibrium [52]. The probability that the newly generated traffic demand on OD w chooses route ρ_w is [53]:

$$\theta_{\rho_w}(t) = \frac{\exp(-\lambda \tau^{\rho_w}(t))}{\sum_{x_w\in\Phi_w} \exp(-\lambda \tau^{x_w}(t))} \tag{23}$$

where $\tau^{\rho_w}(t)$ and $\tau^{x_w}(t)$ denote the total traveling time spent on routes ρ_w and x_w, respectively, for the newly generated traffic flow on OD w; λ is the logit model parameter that indicates the drivers' knowledge of the mixed network travel time.

IV. Cooperative Control

Based on the mixed network traffic model, this section proposes an MPC-based cooperative control model to minimize overall network congestion. The control measures adopted in this study include PC, RM, and VSL, and the corresponding impacts of the control inputs on the traffic flow have been integrated into the above traffic model. Minimizing the TTS of vehicles in the mixed network as the objective function. For convenience, the accumulation of vehicles in the entire expressway network is described as:

$$AEN(t) = \sum_{i\in R}\sum_{j\in\beta_i} L_s \begin{bmatrix} \sum_{l_{ij}=1}^{L_{ij}} K_{E_{ij},l_{ij}}(t) + K_{iE_{ij}}(t) \\ +K_{E_{ij}j}(t) + \sum_{h\in\beta_i} K_{E_{hi}E_{ij}}(t) \end{bmatrix} \tag{24}$$

Thus, the MPC problem at every control step is formulated as follows:

$$J = \min T_s \sum_{t=0}^{T-1} \left(\sum_{i\in R} n_i(t) + AEN(t) \right) \tag{25a}$$

$$\text{s.t } .0 \le u_{ij}(t), \mu_{iE_{ij}}(t) \le 1 \tag{25b}$$

$$V_{\min} \le \eta_{E_{ij}}(t) \le V_{fm} \tag{25c}$$

$$\left|\eta_{E_{ij}}(t) - \eta_{E_{ij}}(t-1)\right| \le \Delta v \tag{25d}$$

$$\eta_{E_{ij}}(t) \bmod 10 = 0 \tag{25e}$$

$$0 \le n_{i,T}(t) \le n_{i,\text{jam}} \tag{25f}$$

where $V_{\min}$ is the minimum speed limit for expressway mainlines; Δv is the maximum speed limit difference between adjacent time steps on the same expressway.

The MPC formulations are detailed: The objective function (25a) incorporates vehicle accumulation in both regions and expressways to minimize overall congestion. Control inputs are bounded by (25b) and (25c). Eq. (25d) restricts the difference between speed limits at adjacent time steps on the same expressway to prevent large fluctuations. Eq. (25e) ensures speed limits are integer multiples of 10 km/h for driver compliance. Lastly, (25f) stipulates that traveling accumulation must not exceed the jam accumulation.

In this paper, we will investigate the effect of these control measures and the combinations between them on improving traffic congestion through the following schemes: (1) no control (NC); (2) PC only; (3) RM and PC (RMPC); (4) VSL and PC (VSLPC) and (5) Cooperative control (CC), i.e., the combination of PC, RM and VSL.

V. Case Studies

A. Network Description and Simulation Setup

In the case studies, a real-world mixed network from the main urban area of Hefei, China, is utilized, covering approximately 214 km^2 with a length of 18.32 km and a width of 11.73 km. The network features a central urban area with traffic gradually dispersing toward the outskirts. The expressway system follows a circular-radial structure, facilitating both regional connectivity and long-distance travel. The network is divided into 7 regions, and the expressway system within this area is extracted and segmented into 10 bidirectional expressways, as shown in Fig. 5. To ensure the accuracy of parameter settings, each region's boundary is determined using OpenStreetMap. Additionally, the MFD for all regions is calibrated through traffic simulation in SUMO, with the production MFD data shown in Fig. 6(a). The average trip lengths of the regions are $\{\bar{L}_i\}=\{3862, 4456, 4552, 4675, 4020, 3748, 3659\}$ m, where$i = 1, 2, \ldots, 7$. Regarding the expressways, the mainline length of each expressway is shown in Table II. The length of a cell is $L_s = 500$ m. The expressway mainline is assumed to have a free-flow speed of 80 km/h and a capacity of 5000 veh/h, while all ramps have a free-flow speed of 40 km/h and a capacity of 2000 veh/h. The capacity decrease parameter $\xi = 0.3$. In simulation and control, the simulation time interval is $T_s = 20$ s, and the control sampling time is 60 s. For the MPC controller, the control horizon is set to 3 and the prediction horizon is set to 9. The logit model parameter λ is set to 0.5. Note

TABLE II
THE MAINLINE LENGTH OF EACH EXPRESSWAY

Expressway	E_{12}/E_{21}	E_{23}/E_{32}	E_{34}/E_{43}	E_{45}/E_{54}	E_{56}/E_{65}	E_{16}/E_{61}	E_{17}/E_{71}	E_{27}/E_{72}	E_{47}/E_{74}	E_{57}/E_{75}
Length(km)	8.0	5.5	6.5	8.0	4.5	5.5	6.5	6.0	7.0	4.0

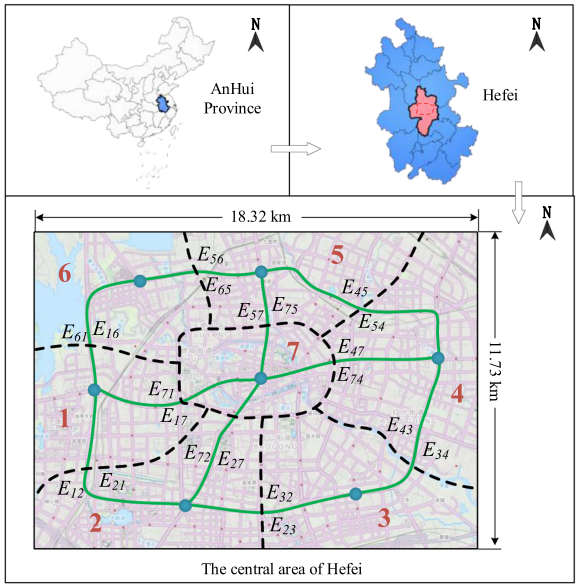

Fig. 5. A real-world mixed network from the urban area of Hefei, China.

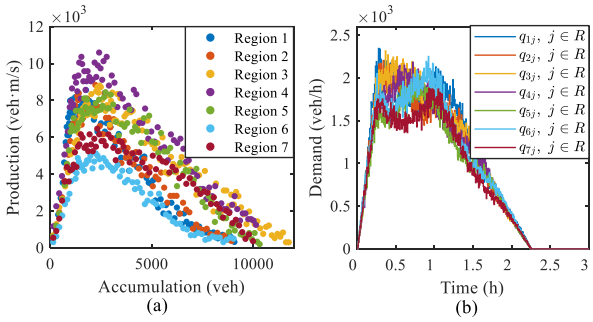

Fig. 6. (a) Trip completion rate in each region, and (b) traffic demand between regional ODs.

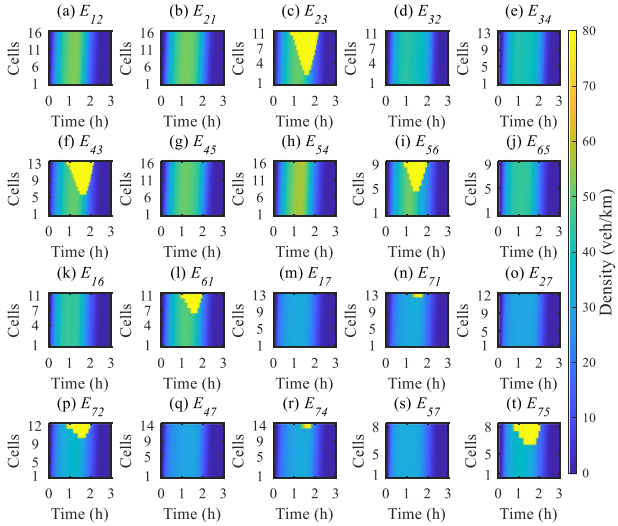

Fig. 7. Density of expressways under the NC scheme.

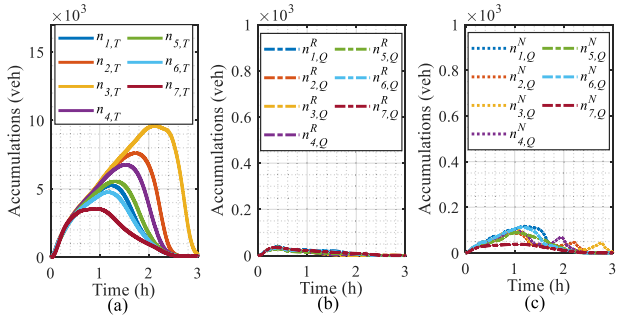

Fig. 8. (a) Traveling accumulation, (b) queuing accumulation at the region boundaries, and (c) queuing accumulation before the on-ramps under the NC scheme.

that to make VSL control more flexible, speed limits are applied only to the last four cells of each expressway mainline. The minimum speed limit is 30 km/h, and the maximum speed limit difference is $\Delta v = 20$ km/h. Finally, the traffic demand, as shown in Fig. 6(b), is adopted to test and compare the proposed control schemes. The control schemes start after the initial 0.5 h traffic loading phase when the vehicle count is low. All experiments were conducted on a desktop machine with a 3.8 GHz AMD Ryzen 7 7840HS processor, 16 GB of memory, and integrated Radeon 780M Graphics. Simulations were carried out using MATLAB R2022b.

B. Control Performance Comparison

We will analyze the state of the mixed network under each control scheme separately and then compare their effectiveness using various traffic indicators. Before that, define the queueing accumulation before the on-ramp in any region i as $n^R_{i,Q}(t) = \sum_\rho \sum_{j\in\alpha_i} n^\rho_{i,Q}(t)\cdot\kappa^\rho_{ij}$, and the queueing accumulation at the boundary in any region i as $n^N_{i,Q}(t) = \sum_\rho \sum_{j\in\beta_i} n^\rho_{i,Q}(t)\cdot\kappa^\rho_{iE_{ij}}$.

1) NC: Fig. 7 shows traffic density on expressways under NC. Fig. 8 displays (a) traveling accumulation, (b) queuing accumulation at region boundaries, and (c) queuing accumulation before on-ramps for each urban region. Regions 1, 5, 6 and 7 are smooth. Regions 2 and 4 have minor congestion, while region 3 faces more severe congestion during peak hours. The average traveling accumulation in urban regions is 23727 vehicles. Without flow control measures, queuing at boundaries is minimal, with the average queuing accumulation of 68 veh at region boundaries and 272 veh before on-ramps.

2) PC: Fig. 9 depicts expressway traffic density under PC. Fig. 10 illustrates (a) traveling accumulation, (b) queuing accumulation at region boundaries, and (c) queuing accumulation

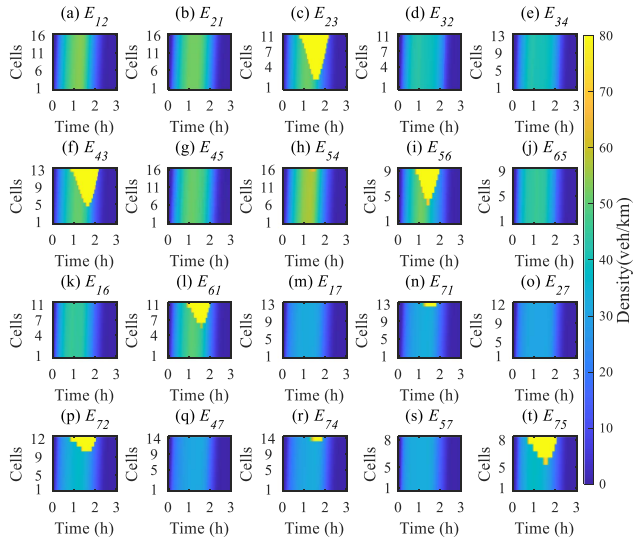

Fig. 9. Density of expressways under the PC scheme.

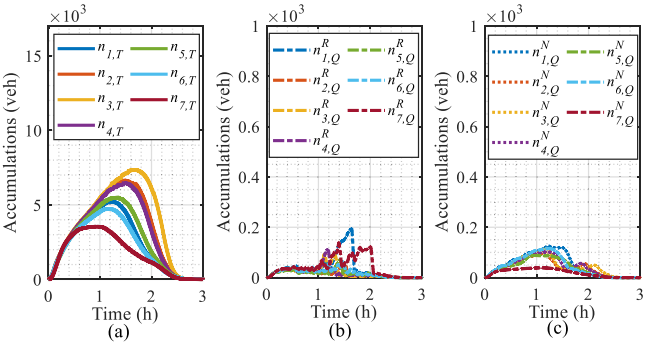

Fig. 10. (a) Traveling accumulation, (b) queuing accumulation at the region boundaries, and (c) queuing accumulation before the on-ramps under the PC scheme.

before on-ramps under PC. Average traveling accumulation decreases to 20471 veh, an 13.72% reduction compared to NC. The average queuing accumulation before on-ramps is 275 veh, similar to NC, while at region boundaries, it increases to 173 veh, which is 1.54 times that in NC.

3) RMPC: Fig. 11 shows expressway density under RMPC. Fig. 12 presents (a) traveling accumulation, (b) queuing accumulation at region boundaries, and (c) queuing accumulation before on-ramps. The average traveling accumulation decreased to 19544 vehicles, a 4.53% reduction from PC. However, on-ramp queuing increases to 561 veh, 1.04 times higher than PC, while region boundary queuing drops to 202 veh, similar to PC. RMPC alleviates regional congestion but significantly increases on-ramp queuing.

4) VSLPC: Fig. 13 shows expressway traffic density under VSLPC. Due to the speed limit control on the mainline, there is a noticeable increase in density in the speed limit sections. Fig. 14 presents (a) traveling accumulation, (b) queuing accumulation at region boundaries, and (c) queuing accumulation before on-ramps. The average traveling accumulation is 18651 veh, a

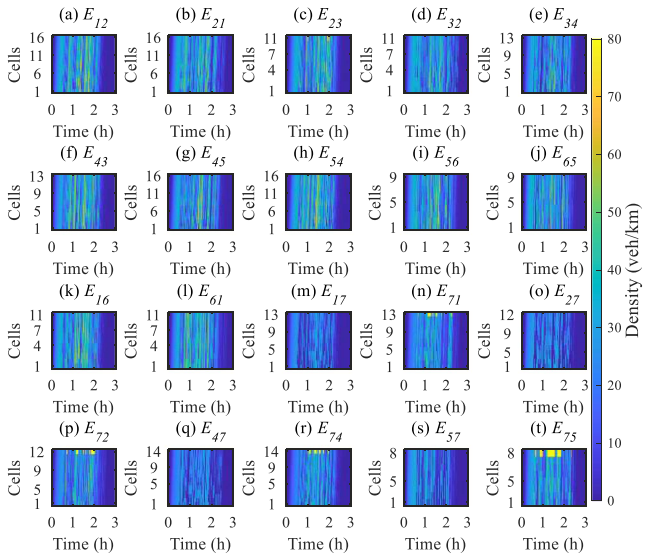

Fig. 11. Density of expressways under the RMPC scheme.

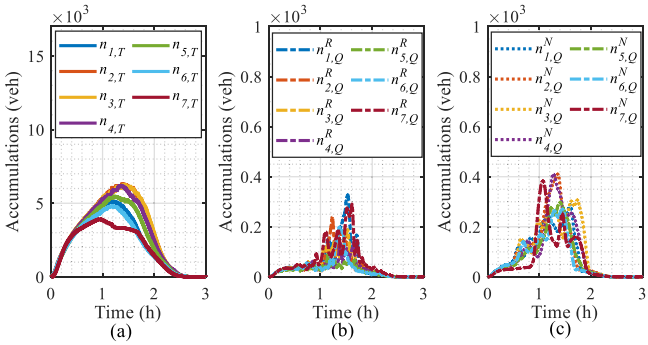

Fig. 12. (a) Traveling accumulation, (b) queuing accumulation at the region boundaries, and (c) queuing accumulation before the on-ramps under the RMPC scheme.

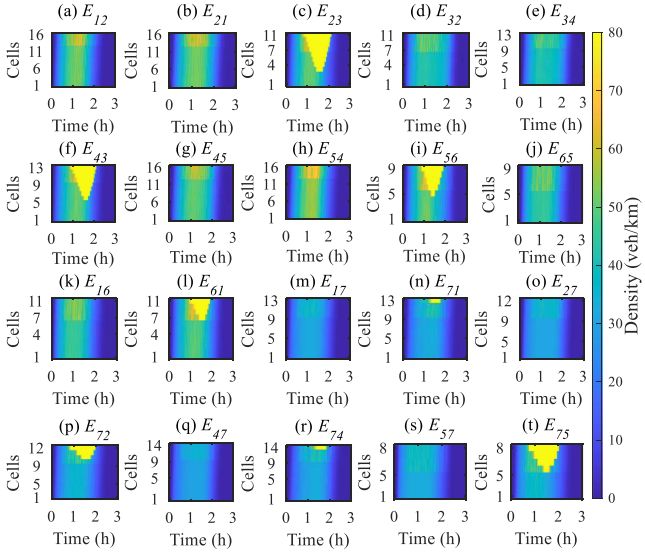

Fig. 13. Density of expressways under the VSLPC scheme.

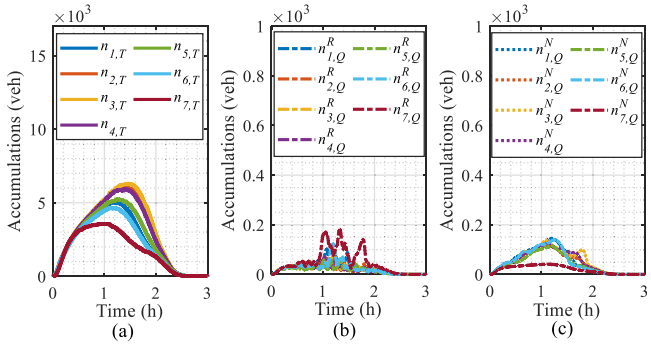

Fig. 14. (a) Traveling accumulation, (b) queuing accumulation at the region boundaries, and (c) queuing accumulation before the on-ramps under the VSLPC scheme.

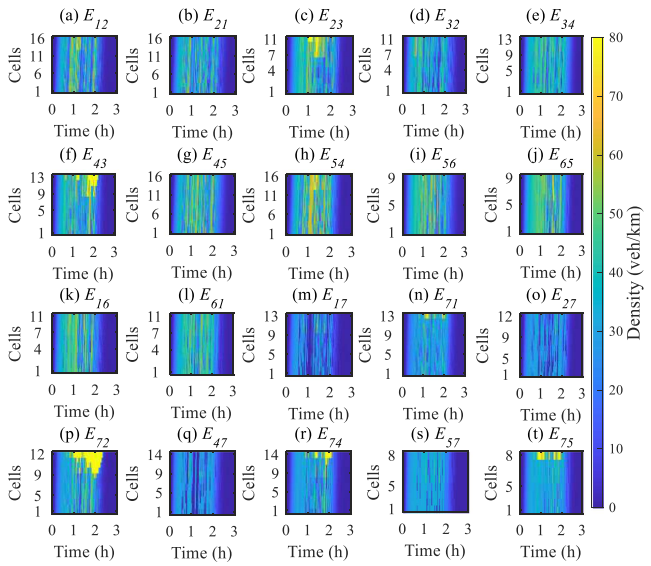

Fig. 15. Density of expressways under the CC scheme.

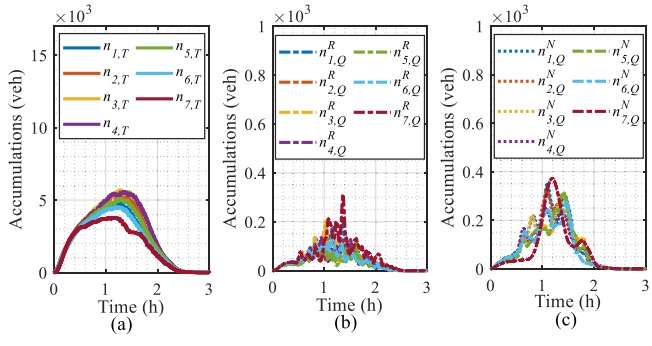

Fig. 16. (a) Traveling accumulation, (b) queuing accumulation at the region boundaries, and (c) queuing accumulation before the on-ramps under the CC scheme.

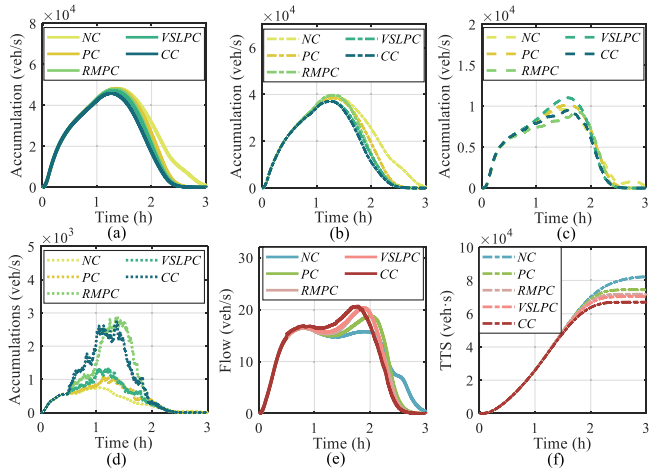

Fig. 17. (a) The accumulation of the whole network, (b) the accumulation of urban regions, (c) the accumulation of the expressway network, (d) total queueing accumulation, (e) total exiting flow, and (f) TTS under different control schemes.

4.57% decrease from RMPC. On-ramp inflow is unrestricted, resulting in an average queuing accumulation before on-ramps of 324 veh, a 42.25% reduction compared to RMPC. Queueing at regional boundaries averages 183 veh, similar to RMPC. The results indicate that VSLPC increases expressway density but reduces urban congestion and queuing compared to RMPC.

5) CC: Fig. 15 shows the expressways density under CC. In the cooperative strategy, both RM and VSL affect the traffic state of the expressway network. Due to the speed limit control, there is a noticeable increase in density in the speed limit sections. Fig. 16 shows (a) traveling accumulation, (b) queuing accumulation at the region boundaries, and (c) queuing accumulation before the on-ramps. The average traveling accumulation in all regions is 17220 veh, which is a 9.33% and 7.67% decrease compared to the RMPC and VSLPC, respectively. The average queueing accumulation before the on-ramps is 431 veh, which is an increase of 33.02% from the VSLPC but a decrease of 23.17% compared to the RMPC. The average queueing accumulation at the regional boundaries is 228 veh, with no significant difference compared to the RMPC and VSLPC. Overall, the CC optimizes the network state by restricting boundary transferring flows and regulating the traffic on the expressway.

We evaluate the effectiveness of control schemes using several traffic indicators and the results are shown in Fig. 17. For clearer and more direct comparisons, these results are summarized in Table III.

Firstly, for the NC, the average accumulation of the whole network is 29720 veh, with 24067 veh in urban regions, 5633 veh on the expressway network, an average queueing accumulation of 340 veh, an average exiting flow of 21.73 veh/s, and a TTS of 82224 veh·s.

After implementing the PC, the average accumulation of the whole network decreases by 10.44% to 26616 veh. The average accumulation in urban regions decreases by 13.08% to 20919 veh. The TTS decreases by 10.44% to 73639 veh·s. However, the average queueing accumulation significantly increases by 31.76% to 448 veh. The average exiting flow increases by 6.68% to 23.18 veh/s.

With the RMPC, the average accumulation of the whole network further reduces by 4.05% to 25539 veh compared to the PC. The average accumulation in urban regions decreases by

TABLE III
THE EVALUATION METRICS UNDER DIFFERENT CONTROL

Control schemes	Avg. accumulation of the whole network (veh)	Avg. accumulation of urban regions (veh)	Avg. accumulation of expressway network (veh)	Avg. queueing accumulations (veh)	Avg. exiting flow (veh/s)	TTS (veh·s)
NC	29,720	24,067	5,653	**340**	21.73	82,224
PC	26,616	20,919	5,697	448	23.18	73,639
RMPC	25,539	20,307	**5,232**	763	23.70	70,657
VSLPC	24,942	19,158	5,784	507	24.23	69,003
CC	**23,630**	**18,379**	5,251	659	**24.90**	**65,374**

2.93% to 20307 veh. The TTS decreases by 4.05%, from 73639 to 70657 veh·s. However, due to ramp metering, the average queueing accumulation significantly increases to 763 veh, an increase of 70.31% compared to the PC. Meanwhile, the average exiting flow increases by 2.23% to 23.70 veh/s.

Next, with the introduction of VSLPC, the average accumulation of the whole network further decreases by 2.34% to 24942 veh compared to RMPC. The average accumulation in urban regions drops to 19158 veh, a 5.66% reduction compared to RMPC. However, the average accumulation on the expressway network increases by 10.55% compared to RMPC, from 5232 to 5784 veh. The TTS is 69003 veh·s, a slight decrease compared to RMPC. The average queueing accumulation drops significantly by 33.55% to 507 veh compared to RMPC, showing a significant improvement. The average exiting flow increases to 24.23 veh/s.

Finally, with the CC, the average accumulation of the whole network is 23630 veh, a reduction of 5.26% compared to VSLPC and 7.48% compared to RMPC. The average accumulation in urban regions is 18379 veh, a reduction of 4.07% compared to VSLPC and 9.50% compared to RMPC, significantly improving traffic flow. The average queueing accumulation increases by 29.98% to 659 veh compared to VSLPC but decreases by 13.63% to RMPC. The TTS decreases to 65374 veh·s, a reduction of 20.49% compared to NC, 7.48% compared to RMPC, and 5.26% compared to VSLPC. The average exiting flow increases to 24.90 veh/s, 2.77% higher than VSLPC and 5.06% higher than RMPC.

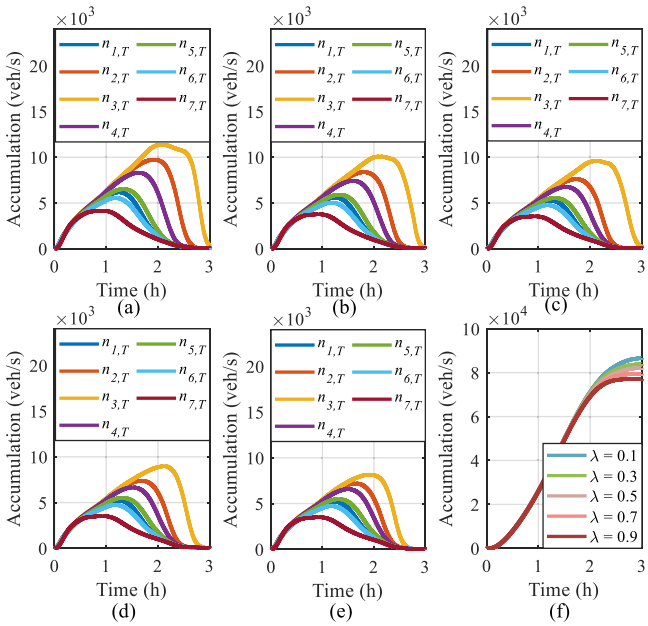

Fig. 18. The traveling accumulation in regions with different values of λ: (a) 0.1, (b) 0.3, (c) 0.5, (d) 0.7, and (e) 0.9; and (f) TTS under different values of λ.

C. Sensitivity Analysis and Computational Efficiency

This section performs sensitivity analyses to investigate the impact of the choice of key parameters on the road network state and computational efficiency.

1) Logit Model Parameter: Firstly, the impact of different λ values in the logit model on network states is examined. In the simulation without control, as λ increases from 0.1 to 0.9 with an interval of 0.1, the traveling accumulations in all regions are shown in Fig. 18(a)–(e). Specifically, as λ increases, the accumulations exhibit a general decreasing trend, while the relative congestion between regions remains consistent. Even with significant changes in λ, the accumulation trends remain stable. This indicates that the model maintains a stable response, demonstrating that the proposed mixed network traffic model has strong robustness in terms of regional adaptability and stability, and can effectively capture network states under different conditions. Fig. 18(f) shows the comparison of TTS at different λ values, with the TTS during the entire simulation period being 86644 veh·s, 83873 veh·s, 82224 veh·s, 79477 veh·s, and 77078 veh·s. The results show that as travelers' ability to perceive traffic conditions improves, traffic congestion in the network is gradually alleviated.

2) MPC Prediction Horizon: The sensitivity analysis of the MPC prediction horizon is conducted while keeping other optimization parameters consistent, where only the prediction horizon is varied under each control scheme. Fig. 19(a) shows the reduction in TTS for each control scheme relative to the NC case at different prediction horizons. Overall, as the prediction horizon increases, the TTS decreases for all control schemes, but the marginal improvement gradually diminishes. For example, with the CC scheme, as the prediction horizon increases from 1 to 9, the TTS reduction increases from 7.93% to 20.49%, but when the prediction horizon is further increased to 15, the TTS only decreases to 21.06%, indicating that the control effect is approaching saturation. A similar pattern is observed for the VSLPC and RMPC schemes. The PC scheme shows the weakest

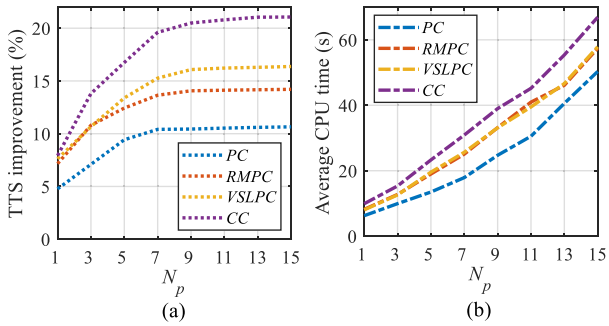

Fig. 19. (a) TTS improvement over NC and (b) average CPU times for each control scheme with varying prediction horizons.

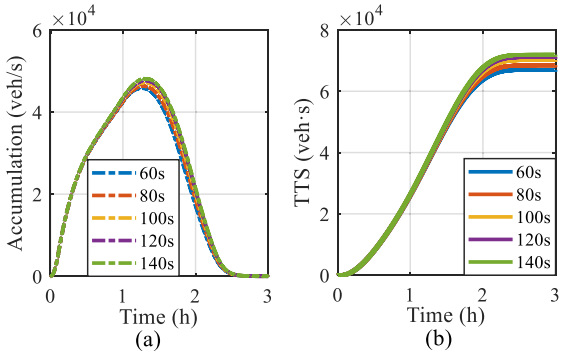

Fig. 20. The total accumulation and the TTS under different control sampling times.

optimization effect, with a reduction of only 10.44% at a prediction horizon of 9, much lower than CC and VSLPC, indicating its limited optimization capability. Overall, CC performs best across all prediction horizons, and by prediction horizon 9, it is close to the optimal value, with further increases in the prediction horizon offering limited improvement.

Additionally, the analysis compares the impact of the prediction horizon on the computational efficiency for each control scheme. Fig. 19(b) shows the average CPU time required for an optimization process at different prediction horizons for each control scheme. It is evident that the CPU time increases significantly as the prediction horizon grows for all schemes. The PC scheme, involving the smallest number of control variables, experiences the slowest increase in CPU time, starting at 6.26 s with a prediction horizon of 1, and rising to 50.33 s at a prediction horizon of 15. In contrast, the CC control scheme, which involves the largest number of control variables, shows the most substantial increase, starting at 9.91 s for a prediction horizon of 1 and increasing to 66.92 s at a prediction horizon of 15. Similarly, both the VSLPC and RMPC schemes exhibit comparable trends, with CPU times reaching 57.87 s and 57.41 s, respectively, at a prediction horizon of 15.

Considering the balance between computational efficiency and optimization performance, although a longer prediction horizon increases the computation time, the corresponding reduction in TTS justifies the additional computational cost. According to the results, the TTS optimization effect for the CC scheme is close to the optimal value at a prediction horizon of 9. Moreover, the average CPU time for the CC strategy at a prediction horizon of 9 is 38.99 s, which is below the 60 s control sampling time requirement of this study, meaning the optimization calculation can be completed within each control cycle. Therefore, choosing a prediction horizon of 9 significantly reduces TTS, effectively controls computational costs, and meets the real-time requirements, making it a reasonable choice.

3) Control Sampling Time: To evaluate the impact of control sampling time on system performance under the CC scheme, a sensitivity analysis is conducted by setting the control sampling time to 60 s, 80 s, 100 s, 120 s, and 140 s, while keeping the prediction horizon at 9 and other parameters unchanged. Fig. 20 illustrates the total accumulation and the TTS over the simulation period under different control sampling times. The results show that as the control sampling time increases, the total accumulation in the mixed network rises, indicating a higher level of congestion. Meanwhile, the TTS increases continuously, reaching 65374 veh·s, 67981 veh·s, 69614 veh·s, 71182 veh·s, and 71922 veh·s, respectively. When the control sampling time extends from 60 s to 140 s, the TTS increases by approximately 10%, reflecting a significant decline in traffic efficiency. This is primarily due to the reduced responsiveness of the system to dynamic traffic conditions, making the control strategy less adaptive to fluctuating demand. Therefore, properly setting the control sampling time is crucial for improving control performance. Considering that the average computation time for each control step in this study is 38.99 s, a sampling time of 60 s is both computationally feasible and capable of achieving relatively optimal control performance under the CC scheme.

VI. Conclusion

This paper proposes a cooperative control method for multiple urban regions traffic flow coupled with an expressway network, focusing on three main aspects. Firstly, a traffic model for the mixed network is established using the MFD and CTM, along with a route choice model. Secondly, a cooperative control method integrating PC, RM, and VSL is proposed within an MPC framework. Finally, case studies compare the effectiveness of different control schemes in addressing congestion in the mixed network.

The analysis of results leads to three key conclusions. First, while the PC scheme is somewhat effective in controlling traffic between regions, it alone cannot alleviate congestion in mixed networks as it does not address expressway traffic inflow into urban regions. Secondly, adopting VSL for expressways is more advantageous than RM when combined with the PC strategy, as expressway mainlines have more storage capacity, reducing urban congestion, ramp queue lengths, and overflow risks. Finally, the CC scheme achieves better coordination between urban and expressway traffic, reducing vehicle accumulation and improving flow rates, proving the necessity of cooperative control strategies in large mixed networks.

Finally, the limitations of this study and directions for future research are discussed. Regarding network construction, this study assumes that each region has only one on-ramp and one off-ramp, which is a simplification. Nevertheless, this assumption still captures the essential structural feature of connections between expressways and urban regions, though it neglects the behavior of vehicles choosing among multiple ramps. On this basis, future research could consider the existence of multiple ramps within each region to enrich the network structure. First, from the perspective of road network design, the number and locations of ramps could be optimized. Then, a ramp selection model could be developed to enable vehicles to flexibly choose ramps according to real-time traffic conditions. With the expansion of urban areas, future research could also focus on designing a more efficient expressway network system by considering factors such as urban growth patterns, traffic demand, and land use, to enhance connectivity. In addition, there is still room for further development in terms of control strategies. Future research can integrate route guidance strategies to dynamically allocate vehicles across alternative routes, thereby fully leveraging the structural advantages of mixed networks and achieving more efficient traffic management.

REFERENCES

[1] Z. C. Li, Y. J. Chen, Y. D. Wang, W. H. Lam, and S. C. Wong, "Optimal density of radial major roads in a two-dimensional monocentric city with endogenous residential distribution and housing prices," *Regional Sci. Urban Econ.*, vol. 43, no. 6, pp. 927–937, 2013.

[2] E. Taillanter and M. Barthelemy, "Evolution of road infrastructure in large urban areas," *Phys. Rev. E*, vol. 107, no. 3, 2023, Art. no. 034304.

[3] T. Li, H. Sun, J. Wu, Z. Gao, Y. E. Ge, and R. Ding, "Optimal urban expressway system in a transportation and land use interaction equilibrium framework," *Transportmetrica A:,Transport Sci.*, vol. 15, no. 2, pp. 1247–1277, 2019.

[4] Y. Yang, M. Li, J. Yu, and F. He, "Expressway bottleneck pattern identification using traffic Big Data—The case of ring roads in Beijing, China," *J. Intell. Transp. Syst.*, vol. 24, no. 1, pp. 54–67, 2020.

[5] T. Oguchi et al., "Traffic management measures on Tokyo metropolitan urban expressway rings," *J. Jpn. Soc. Civil Engineers*, vol. 74, no. 5, pp. 1255–1263, 2018.

[6] J. Jin, Y. Li, H. Huang, Y. Dong, and P. Liu, "A variable speed limit control approach for freeway tunnels based on the model-based reinforcement learning framework with safety perception," *Accident Anal. Prevention*, vol. 201, 2024, Art. no. 107570.

[7] B. Zhai, Y. Wang, B. Wu, and W. Wang, "Adaptive control strategy of variable speed limit on freeway segments under fog conditions," *J. Transp. Eng., Part A, Syst.*, vol. 149, no. 10, 2023, Art. no. 04023097.

[8] Y. Di, W. Zhang, H. Ding, X. Zheng, and H. Bai, "Integrated control for mixed CAV and CV traffic flow in expressway merge zones combined with variable speed limit, ramp metering, and lane changing," *J. Transp. Eng., Part A, Syst.*, vol. 149, no. 2, 2023, Art. no. 04022140.

[9] Z. He, L. Wang, Z. Su, and W. Ma, "Integrating variable speed limit and ramp metering to enhance vehicle group safety and efficiency in a mixed traffic environment," *Physica A, Stat. Mechan. Appl.*, vol. 641, 2024, Art. no. 129754.

[10] Q. Lin, W. Huang, Z. Wu, M. Zhang, and Z. He, "Multi-agent game theory-based coordinated ramp metering method for urban expressways with multi-bottleneck," *IEEE Trans. Intell. Transp. Syst.*, vol. 26, no. 3, pp. 3643–3658, Mar. 2025.

[11] C. F. Daganzo, "Urban gridlock: Macroscopic modeling and mitigation approaches," *Transp. Res. Part B, Methodological*, vol. 41, no. 1, pp. 49–62, 2007.

[12] N. Geroliminis and C. F. Daganzo, "Existence of urban-scale macroscopic fundamental diagrams: Some experimental findings," *Transp. Res. Part B, Methodological*, vol. 42, no. 9, pp. 759–770, 2008.

[13] G. Mariotte, L. Leclercq, and J. A. Laval, "Macroscopic urban dynamics: Analytical and numerical comparisons of existing models," *Transp. Res. Part B, Methodological*, vol. 101, pp. 245–267, 2017.

[14] J. Haddad and Z. Zheng, "Adaptive perimeter control for multi-region accumulation-based models with state delays," *Transp. Res. Part B, Methodological*, vol. 137, pp. 133–153, 2020.

[15] W. L. Jin, "Generalized bathtub model of network trip flows," *Transp. Res. Part B, Methodological*, vol. 136, pp. 138–157, 2020.

[16] C. Chen, N. Geroliminis, and R. Zhong, "An iterative adaptive dynamic programming approach for macroscopic fundamental diagram-based perimeter control and route guidance," *Transp. Sci.*, vol. 58, no. 4, pp. 896–918, 2024.

[17] H. Fu, S. Chen, K. Chen, A. Kouvelas, and N. Geroliminis, "Perimeter control and route guidance of multi-region MFD systems with boundary queues using colored petri nets," *IEEE Trans. Intell. Transp. Syst.*, vol. 23, no. 8, pp. 12977–12999, Aug. 2022.

[18] Y. Qian, H. Ding, Y. Meng, N. Zheng, Y. Di, and X. Zheng, "Combination of H∞ perimeter control and route guidance for heterogeneous urban road networks," *Transportmetrica B, Transport Dyn.*, vol. 12, no. 1, 2024, Art. no. 2359025.

[19] C. Chen, N. Geroliminis, and R. Zhong, "An iterative adaptive dynamic programming approach for macroscopic fundamental diagram-based perimeter control and route guidance," *Transp. Sci.*, vol. 58, pp. 896–918, 2024.

[20] N. Zheng, G. Rérat, and N. Geroliminis, "Time-dependent area-based pricing for multimodal systems with heterogeneous users in an agent-based environment," *Transp. Res. Part C, Emerg. Technol.*, vol. 62, pp. 133–148, 2016.

[21] A. Loder, M. C. Bliemer, and K. W. Axhausen, "Optimal pricing and investment in a multi-modal city—Introducing a macroscopic network design problem based on the MFD," *Transp. Res. Part A, Policy Pract.*, vol. 156, pp. 113–132, 2022.

[22] Z. Gu, S. Shafiei, Z. Liu, and M. Saberi, "Optimal distance-and time-dependent area-based pricing with the network fundamental diagram," *Transp. Res. Part C, Emerg. Technol.*, vol. 95, pp. 1–28, 2018.

[23] Z. He, Y. Han, X. Ji, H. Yu, P. Liu, and A. Kouvelas, "Hierarchical perimeter control with network heterogeneity reduction and queue management," *IEEE Intell. Transp. Syst. Mag.*, vol. 16, no. 5, pp. 46–67, Sep./Oct. 2024.

[24] H. Ding, Y. Di, Z. Feng, W. Zhang, X. Zheng, and T. Yang, "A perimeter control method for a congested urban road network with dynamic and variable ranges," *Transp. Res. Part B, Methodological*, vol. 155, pp. 160–187, 2022.

[25] X. Li, X. Zhang, X. Qian, C. Zhao, Y. Guo, and S. Peeta, "Beyond centralization: Non-cooperative perimeter control with extended mean-field reinforcement learning in urban road networks," *Transp. Res. Part B, Methodological*, vol. 186, 2024, Art. no. 103016.

[26] W. Ma, P. Li, J. Zhao, J. Qi, and C. Li, "Organized traffic interweaving: Cooperative trajectory control of vehicles merging from exit ramps onto surface streets," *J. Transp. Eng., Part A, Syst.*, vol. 151, no. 3, 2025, Art. no. 04024119.

[27] M. Deng, F. Chen, Y. Gong, X. Li, and S. Li, "Optimization of signal timing for urban expressway exit ramp connecting intersection," *Sensors*, vol. 23, no. 15, 2023, Art. no. 6884.

[28] D. Su, X. Y. Lu, R. Horowitz, and Z. Wang, "Coordinated ramp metering and intersection signal control," *Int. J. Transp. Sci. Technol.*, vol. 3, no. 2, pp. 179–192, 2014.

[29] Z. Xu, Y. Zheng, and Y. Li, "Coordinated control of urban expressways and connecting intersection based on genetic algorithm," in *Proc. 9th Int. Conf. Comput. Commun. Syst.*, 2024, pp. 1132–1138.

[30] A. A. Farabi, R. Mohebifard, R. Niroumand, A. Hajbabaie, M. Hadi, and L. Elefteriadou, "Integrated corridor management by cooperative traffic signal and ramp metering control," *Comput.-Aided Civil Infrastructure Eng.*, vol. 39, pp. 2439–2456, 2024.

[31] C. F. Daganzo, "The cell transmission model: A dynamic representation of highway traffic consistent with the hydrodynamic theory," *Transp. Res. Part B, Methodological*, vol. 28, no. 4, pp. 269–287, 1994.

[32] J. Haddad, M. Ramezani, and N. Geroliminis, "Cooperative traffic control of a mixed network with two urban regions and a freeway," *Transp. Res. Part B, Methodological*, vol. 54, pp. 17–36, 2013.

[33] H. Ding, H. Yuan, X. Zheng, H. Bai, W. Huang, and C. Jiang, "Integrated control for a large-scale mixed network of arterials and freeways," *IEEE Intell. Transp. Syst. Mag.*, vol. 13, no. 3, pp. 131–145, Fall 2021.

[34] X. Wang and V. V. Gayah, "Cordon-based pricing schemes for mixed urban-freeway networks using macroscopic fundamental diagrams," *Transp. Res. Rec.*, vol. 2675, no. 10, pp. 1339–1351, 2021.

[35] P. K. Barik, K. Munjpara, A. Gevariya, H. Mangukiya, M. Kotadiya, and N. Mulani, "Density-based automatic traffic control using machine learning," in *Proc. IEEE 11th Region 10 Humanitarian Technol. Conf.*, 2023, pp. 97–102.
[36] J. Azimjonov, A. Özmen, and T. Kim, "A nighttime highway traffic flow monitoring system using vision-based vehicle detection and tracking," *Soft Comput.*, vol. 27, no. 19, pp. 13843–13859, 2023.
[37] M. F.-Sanjurjo, B. Bosquet, M. Mucientes, and V. M. Brea, "Real-time visual detection and tracking system for traffic monitoring," *Eng. Appl. Artif. Intell.*, vol. 85, pp. 410–420, 2019.
[38] S. Khan, H. Ali, Z. Ullah, and M. F. Bulbul, "An intelligent monitoring system of vehicles on highway traffic," in *Proc. 12th Int. Conf. Open Source Syst. Technol.*, 2018, pp. 71–75.
[39] G. Han, X. Liu, Y. Han, X. Peng, and H. Wang, "CycLight: Learning traffic signal cooperation with a cycle-level strategy," *Expert Syst. Appl.*, vol. 255, 2024, Art. no. 124543.
[40] D. Shaheen, G. J. L. Paulraj, I. J. Jebadurai, and S. Kirubakaran, "Intelligent traffic management system using multi-agent reinforcement learning," in *Proc. 2025 Int. Conf. Electron. Renewable Syst.*, 2025, pp. 1975–1981.
[41] G. Han, Y. Han, H. Wang, T. Ruan, and C. Li, "Coordinated control of urban expressway integrating adjacent signalized intersections using adversarial network based reinforcement learning method," *IEEE Trans. Intell. Transp. Syst.*, vol. 25, no. 2, pp. 1857–1871, Feb. 2024.
[42] L. N. Alegre, T. Ziemke, and A. L. C. Bazzan, "Using reinforcement learning to control traffic signals in a real-world scenario: An approach based on linear function approximation," *IEEE Trans. Intell. Transp. Syst.*, vol. 23, no. 7, pp. 9126–9135, Jul. 2022.
[43] Z. Hu and W. Ma, "Guided deep reinforcement learning for coordinated ramp metering and perimeter control in large scale networks," *Transp. Res. Part C, Emerg. Technol.*, vol. 159, 2024, Art. no. 104461.
[44] H. Ding, Y. Meng, N. Zheng, X. Zheng, W. Huang, and C. Qin, "Ramp layout optimization and integrated control for mixed networks of freeways and arterial roads in an intelligent connected vehicle environment," *Transp. Res. Part C, Emerg. Technol.*, vol. 176, 2025, Art. no. 105124.
[45] Y. Y. Chen, Y. H. Chen, and G. L. Chang, "Optimizing the integrated off-ramp signal control to prevent queue spillback to the freeway mainline," *Transp. Res. Part C, Emerg. Technol.*, vol. 128, 2021, Art. no. 103220.
[46] Y. Li, R. Mohajerpoor, and M. Ramezani, "Perimeter control with real-time location-varying cordon," *Transp. Res. Part B, Methodological*, vol. 150, pp. 101–120, 2021.
[47] J. Haddad, "Optimal coupled and decoupled perimeter control in one-region cities," *Control Eng. Pract.*, vol. 61, pp. 134–148, 2017.
[48] A. Ferrara, S. Sacone, and S. Siri, *Freeway Traffic Modelling and Control*, vol. 585. Berlin, Germany: Springer, 2018.
[49] Y. Han, A. Hegyi, Y. Yuan, S. Hoogendoorn, M. Papageorgiou, and C. Roncoli, "Resolving freeway jam waves by discrete first-order model-based predictive control of variable speed limits," *Transp. Res. Part C, Emerg. Technol.*, vol. 77, pp. 405–420, 2017.
[50] Z. Li, P. Liu, C. Xu, and W. Wang, "Optimal mainline variable speed limit control to improve safety on large-scale freeway segments," *Comput.-Aided Civil Infrastructure Eng.*, vol. 31, no. 5, pp. 366–380, 2016.
[51] N. Moshahedi and L. Kattan, "Alpha-fair large-scale urban network control: A perimeter control based on a macroscopic fundamental diagram," *Transp. Res. Part C, Emerg. Technol.*, vol. 146, 2023, Art. no. 103961.
[52] F. Hosseinzadeh, N. Moshahedi, and L. Kattan, "An MFD approach to route guidance with consideration of fairness," *Transp. Res. Part C, Emerg. Technol.*, vol. 157, 2023, Art. no. 104359.
[53] J. N. Prashker and S. Bekhor, "Route choice models used in the stochastic user equilibrium problem: A review," *Transport Rev.*, vol. 24, no. 4, pp. 437–463, 2004.

Yunran Di received the B.Eng. degree from the North China University of Technology, Beijing, China, in 2014, and the M.S. degree in 2018 from the School of Automotive and Transportation Engineering, Hefei University of Technology, Hefei, China, where he is currently working toward the Ph.D. degree in engineering. He was a Visiting Scholar with the University of Wisconsin-Madison, Madison, WI, USA. His research interests include regional road network traffic modeling and traffic control.

Weihua Zhang is currently a Professor with the School of Automotive and Transportation Engineering, Hefei University of Technology, Hefei, China. His research interests include the theory and method of regional and urban transportation system planning, the basic theory and method of intelligent transportation system, traffic environment, and traffic safety. He has authored or coauthored more than 70 academic papers in core or important academic journals and academic conferences.

Heng Ding is currently a Professor with the School of Automotive and Transportation Engineering, Branch Secretary of the Department of Road and Traffic Engineering, and the Deputy Director of the Institute of Traffic Engineering, Hefei University of Technology, Hefei, China. His research interests include traffic management and control, intelligent measurement, control technology and application.

Haotian Shi received the Ph.D. degree in civil and environmental engineering from the University of Wisconsin-Madison, Madison, WI, USA, in 2023. He is currently a Research Associate with the University of Wisconsin-Madison. His main research interests include prediction/control of connected automated vehicles, intelligent transportation systems, traffic crash data analysis, and deep reinforcement learning.

Junwei You received the M.S. degree in civil and environmental engineering from Northwestern University, Evanston, IL, USA, in 2022. He is currently working toward the Ph.D. degree in civil and environmental engineering with the University of Wisconsin–Madison, Madison, WI, USA. His research interests include multimodal generative AI, connected and automated vehicles, and deep learning advancement in intelligent transportation systems.

Hangyu Li (Graduate Student Member, IEEE) received the B.Eng. degree in vehicle engineering from Tsinghua University, Beijing, China, in 2021, and the M.Phil. degree in intelligent transportation from the Hong Kong University of Science and Technology, Hong Kong SAR, China, in 2023. He is currently working toward the Ph.D. degree with the University of Wisconsin-Madison, Madison, WI, USA under Prof. Xiaopeng Li. His research focuses on automation and cooperation in intelligent transportation systems.

Bin Ran is currently a Vilas Distinguished Achievement Professor and the Director of ITS Program with the University of Wisconsin at Madison, Madison, WI, USA. He is an expert in dynamic transportation network models, traffic simulation and control, traffic information system, internet of mobility, and Connected Automated Vehicle Highway (CAVH) System. He has coauthored more than 240 journal papers and more than 260 referenced papers at national and international conferences. He holds more than 20 patents of CAVH in the US and other countries. He is an Associate Editor for *Journal of Intelligent Transportation Systems*.